in CON, reflected in an increased MO2ex ($P<0.05$), while it had no effect in DM+HFD+CKD, suggesting that loss of NO was principally responsible for the perturbation in myocardial oxygen delivery in DM+HFD+CKD (Figure). This was supported by lower myocardial levels of NO2-+NO3- in DM+HFD+CKD compared to CON (0.20±0.02 vs 0.34±0.06 µmol/mg protein, $P<0.05$). Isolated vessels of DM+HFD+CKD swine showed decreased endothelial dependent vasodilation to BK, mediated via a complete abolishment of the NO-dependent vasodilator pathway, consistent with the in vivo observations.

Conclusion: Prolonged exposure to DM, HFD and CKD results in a pro-inflammatory state associated with impaired coronary microvascular NO production, thereby altering coronary microvascular dilation and hampering myocardial perfusion.

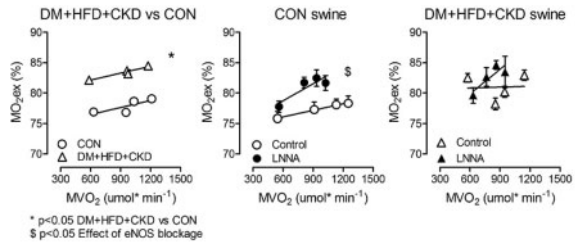

Abstract P550 Figure. Myocardial Oxygen Balance

P551

Effects of interferon gamma on endothelial barrier function: differential role of classical and non-classical pathways

S. Mahmood[1]; N. Sevinc[1]; C. Troidl[1]; R. Schulz[2]; B. Schiefer[3]; C. Tanislav[4]; D. Guenduez[1]; CW. Hamm[1]; M. Aslam[1]
[1]University Hospital Giessen and Marburg, Medical Clinic I, Cardiology and Angiology, Giessen, Germany; [2]Institute of Physiology, Justus Liebig University, Giessen, Germany; [3]University Hospital Giessen and Marburg, Cardiology and Angiology, Marburg, Germany; [4]University Hospital Giessen and Marburg, Department of Neurology, Giessen, Germany

Background: Increased vascular permeability is a surrogate marker for the development of atherosclerotic lesions. Loss of EC barrier integrity exposes the underlying interstitium to a variety of cytokines present in the blood creating a local inflammatory microenvironment which harbours more inflammatory cells. During the progression of atherosclerosis the expression of several cytokines including interferon gamma (IFN-g) is upregulated. The role of IFN-g in the development and progression of atherosclerosis is increasingly debated due to the presence of evidence conveying both pro- and anti- atherogenic actions of IFN-g. While EC activation and loss of their integrity is one of the major factors contributing towards progression of atherosclerosis, little is known about its effects on EC barrier function and related signalling.
Methods: The study was carried out on cultured human umbilical vein endothelial cells (ECs) and rat coronary microvascular ECs. Endothelial barrier function was analysed by measuring the flux of albumen through EC monolayers cultured on filter membranes. Gene expression was analysed by qPCR-based assays.
Results: Quantitative PCR analysis showed that ECs express both IFNGR1 and IFNGR2. Chronic treatment of confluent EC monolayers with IFN-g (40 ng/mL) for 48h attenuated thrombin-induced EC hyper-permeability, actin cytoskeleton remodelling, and loss of cell-cell junctions ($n=5$; $p<0.05$). Thrombin-induced a robust activation of RhoA, Rho kinase, and phosphorylation of myosin light chain (MLC; a marker of EC contractile activation) which was significantly attenuated in EC monolayers pre-treated with IFN-g. Likewise, adhesion of freshly isolated human monocytes was significantly reduced on EC monolayers pre-treated with IFN-g. In next step, ECs were primed towards classical IFN-g-stat1 signalling pathway by short term pre-treatment with PDGF (10 ng/mL; 3h). Surprisingly, priming of ECs towards classical IFN-g signalling resulted in loss all IFN-g-mediated protective effects on endothelial barrier function, contractile activation and cell-cell junction. Likewise, IFN-g transformed the PDGF-primed endothelial monolayers towards inflamed condition resulting in massive adhesion of non-activated monocytes.
Conclusion: The data of the present study demonstrate that the effects of IFN-g on endothelial monolayers is dependent upon the basal state of ECs. In non-primed ECs IFN-g exerts endothelial barrier protective effect while in ECs primed for classical pathway, IFN-g has barrier disruptive and pro-inflammatory effects.

P552

Role of PI3K/Akt and MEK/ERK signalling in Epac-mediated endothelial barrier stabilisation and survival

N. Sevinc[1]; C. Troidl[1]; C. Tanislav[2]; D. Guenduez[1]; CW. Hamm[1]; M. Aslam[1]
[1]University Hospital Giessen and Marburg, Medical Clinic I, Cardiology and Angiology, Giessen, Germany; [2]University Hospital Giessen and Marburg, Department of Neurology, Giessen, Germany

Background and Aims: Activation of the cAMP/Epac signalling stabilises endothelial barrier function. cAMP/Epac also activates PI3K/Akt and MEK/ERK signalling in diverse cell types, but the impact of this activation on endothelial barrier function is largely unknown. Here the role of PI3K/Akt and MEK/ERK signalling in cAMP/Epac-mediated endothelial barrier stabilisation was analysed.
Methods: Endothelial barrier function was analysed in cultured human umbilical vein endothelial cells (HUVECs) by measuring albumin flux. A modified cAMP analogue 8-pCPT-2'-O-Me-cAMP was used to specifically activate cAMP/Epac signalling. Activation of PI3K, Akt, MEK, and ERK was measured by Western blotting. Caspase activity was determined by Caspase-Glo kit. qPCR was used to quantify the expression level of PI3K isoforms. Cytoskeletal proteins and cell-cell junctions were visualised by immunohistochemistry using phalloidin TRITC and antibody against VE-cadherin, respectively. Endothelial cell proliferation was determined by expression of Ki67.
Results: The Epac agonist reduced basal and attenuated thrombin-induced endothelial hyperpermeability; this was accompanied by an activation of PI3K/Akt and MEK/ERK signalling. qPCR demonstrated that HUVECs express PI3Kα, PI3Kβ, and PI3Kγ but not PI3Kδ isoforms. Western blotting confirmed that the Epac agonist preferentially activates PI3Kα and PI3Kβ isoforms. Inhibition of the MEK/ERK using U0126 but not the PI3K/Akt pathway by Akt inhibitor VIII, potentiated the endothelial barrier-protective effects of cAMP/Epac signalling. Inhibition of MEK/ERK signalling in the presence of the Epac agonist induced reorganisation of the actin cytoskeleton to the cell periphery, reduced stress fibre formation, and enhanced VE-cadherin localisation at cell-cell junctions. Moreover, the Epac agonist promoted endothelial cell (EC) survival but not proliferation via reduction in activities of pro-apoptotic caspases in a PI3K/Akt and MEK/ERK signalling-dependent manner as determined by respective selective pharmacological inhibitors.
Conclusion: Our data demonstrate that stimulation of the cAMP/Epac axis simultaneously activates PI3K/Akt and MEK/ERK pathways, which govern the pro-survival effects of Epac signalling on ECs. Inhibition of MEK/ERK but not PI3K/Akt signalling enhances barrier-stabilising and barrier-protective effects of cAMP/Epac activation.

P553

H2S donor (NaHS) restores endothelium-dependent relaxation of smooth muscles in old rats

K. Drachuk; VF. Sagach
Bogomoletz Institute of Physiology, Kiev, Ukraine

Background: The effects of H2S donor (NaHS) on indicators of oxidative/nitrosative stress, coupling of constitutive NO-synthase (cNOS) and endothelium-dependent relaxation of smooth muscles (SM) in old rats were studied.
Methods: Endothelium-dependent relaxation of SM was performed on isolated thoracic aorta by the conventional method in a mode close to isotonic. The markers of oxidative/nitrosative stress (the rate of $O2\bullet^-$, $\bullet OH$ generation, pools of H2O2, the activity of iNOS, NO3- pools) and constitutive NO-synthesis (activity of cNOS and NO2- pools) were determined in aorta tissue by spectrophotometric method. The index of cNOS coupling was calculated as cNOS activity related to the rate of $O2\bullet^-$generation.
Main results. It was found that old rats had impairment endothelium-dependent relaxation of SM (7.5 ± 1.4%, compared with 64.9 ± 3.5% in adults). This functional disorder was accompanied by a decrease of H2S pools (by 1.6 times). It has been also revealed that a combined oxidative and nitrosative stress was developed, leading to cNOS uncoupling (the index of cNOS coupling was decreased by 20 times) and decline of the constitutive NO synthesis (cNOS activity and NO2- pools were decreased by 3 and 1.7 times, respectively).
It has been shown, that NaHS, improved endothelium-dependent relaxation of SM (48.8 ± 1.9%, compared with 7.5 ± 1.4% in intacted old rats). The molecular mechanisms of NaHS action included the increase of H2S pools (by 2 times), inhibition of the oxidative/nitrosative stress, restoration of the cNOS coupling and reduction of the constitutive NO synthesis.
Conclusions: Thus, NaHS recovers endothelium-dependent relaxation of SM in old rats via oxidative/nitrosative stress inhibition, cNOS recoupling and constitutive synthesis of NO stimulation.

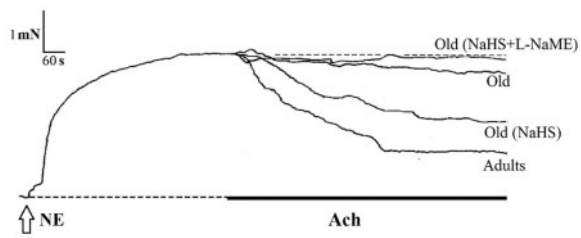

Abstract P553 Figure. NaHS & endothelium-dependent relaxation

P554

Characterization of RNA-rich platelets by means of Cell Sorting and RNA-Sequencing

L. Hille[1]; M. Cederqvist[1]; C. Stratz[1]; B. Gruening[2]; V. Benes[3]; L. Hein[4]; F-J Neumann[1]; D. Trenk[1]; T. Nuehrenberg[1]
[1]Universitäts-Herzzentrum Freiburg - Bad Krozingen, Klinik für Kardiologie und Angiologie II, Bad Krozingen, Germany; [2]University of Freiburg, Department of Bioinformatics, Freiburg, Germany; [3]EMBL, Genomics Core Facility, Heidelberg, Germany; [4]Universität Freiburg, Institut für experimentelle und klinische Pharmakologie und Toxikologie, Freiburg, Germany

Background: Reticulated platelets (RP), also named immature platelets, are a fraction of the platelet pool, representing the youngest platelets released from the bone marrow. They are characterized by distinct features comprising increased ribonucleic acid content, greater volume, more dense granules, higher levels of surface activation markers and probably higher platelet reactivity. To date, several studies have shown an association of RP levels and cardiovascular events or mortality. The current study sought to investigate qualitative differences in the RNA content of RNA-rich versus RNA-low platelets in order to determine potential causes for their specific properties.
Methods: Citrate-anticoagulated blood samples were obtained from three healthy donors on two different days. Washed platelets were prepared and stained with SYTO® 13, a highly specific nucleic acid binding fluorescent dye. At the borders of the continuum of all platelets containing RNA, two gates representing the 20% of platelets with highest staining intensity (RNA-rich platelets) and the 20% of platelets with lowest staining intensity (RNA-low platelets) were used to sort

platelets based on their RNA-amount. Given the non-linear time-dependent RNA decay and the platelet lifespan of 8 to 10 days, RNA-rich platelets contain the youngest platelets, whereas RNA-low platelets constitute a population at the end of the platelet lifespan. After RNA extraction, RNA yield was measured by Bioanalyzer®. After preparation of libraries for long and small RNAs, Illumina Next Generation Sequencing was performed. Sequenced reads were analyzed by use of the local Galaxy platform. Differential gene expression and gene ontologies were assessed with DESeq2 and ClueGO, respectively.

Results: RNA quantity measurement resulted in a median RNA amount of 0.52 [0.33 – 0.68] fg per platelet in RNA-low platelets and 1.04 [0.67 – 1.15] fg per platelet in RNA-rich platelets.

Long RNA sequencing revealed 131 significantly enriched genes in RNA-rich platelets (adjusted $p < 0.05$ FDR by Benjamini-Hochberg correction) and 78 enriched genes in RNA-low platelets. Gene ontology analysis yielded 36 GO-terms for genes with increased expression in RNA-rich platelets – particularly genes which are responsible for platelet reactivity, shape change, clotting and cell-cell-interactions. Only 1 GO-term -'vesicle docking for exocytosis'- was found for genes enriched in RNA-low platelets.

Small RNA sequencing showed no significant up- or downregulation in sequenced genes of the examined platelet populations.

Conclusion: RNA-sequencing of RNA-low and RNA-rich platelets indicated notable changes in transcripts of protein-coding genes. Especially gene clusters involved in platelet reactivity are enriched in RNA-rich platelets.Given the fact that RNA-rich platelets seem to play an important role in numerous cardiovascular diseases, enrichment of associated transcripts deserves further study.

Abstract P554 Figure.

P555

Pannexin1 promotes hemostasis and thrombosis by warranting platelet function

F. Molica; MJ. Meens; Y. Emre; G. Pelli; BA. Imhof; BR. Kwak
University of Geneva, Pathology and Immunology, Geneva, Switzerland

Background: Platelets accumulate at sites of vessel injury to prime hemostasis. This event may occur excessively in atherosclerotic lesions, leading to acute ischemic events. Previous studies report that ATP release through Pannexin1 (Panx1) membrane channels contributes to human platelet aggregation in vitro, which was supported by the association between a Panx1-400A>C gain-of-function genetic polymorphism and collagen-induced platelet reactivity in a small cohort of healthy subjects.

Aim: Here, we investigate the effects of genetic or pharmacological reduction of Panx1 channel function on platelet aggregation in vitro and in vivo.

Methods: : Aggregation responses of WT or Panx1-/ platelets to collagen or arachidonic acid (AA) were measured by turbidimetry. Alternatively, platelets were pre-incubated during 7 min with the Panx1 inhibitor Brilliant Blue FCF (BB-FCF). To study the effects of Panx1 deficiency on hemostasis and thrombosis, we used mice with ubiquitous (Panx1-/-) or specific deletion of Panx1 in platelets (Pf4-CreTgPanx1fl/fl). In vivo bleeding time was assessed on tails, FeCl3-induced arterial thrombosis on mesenteric arteries and venous thromboembolism after injection of a collagen/epinephrine mixture in the jugular vein. Vasomotor function was measured by wire myography on mesenteric arteries.

Results: Panx1 channel function blockade with 1 mM of the food dye BB-FCF or Panx1 deletion specifically reduced in vitro platelet aggregation induced by 1 µg/mL collagen as compared to control conditions. The aggregation response induced by AA (75 µM) was not affected. Panx1 deficiency also delayed hemostasis; bleeding time after tail transection was increased in Panx1-/- mice compared with WT controls (788±76 vs 308±62 s, respectively. n=8). Vasoconstriction induced by phenylephrine (10 mM), KCl (10 mM), U446619 (10 nM) or endothelin-1 (10 nM) was decreased also in Panx1-/- mice, partly explaining the decreased hemostatic response. However, bleeding time was also increased in Pf4-CreTgPanx1fl/fl mice compared with Panx1fl/fl mice (536±121 vs 246±37 s, respectively. n=7-9). Time to circulatory arrest after FeCl3-induced vessel wall injury in mesenteric arteries was slightly increased in Pf4-Cre+Panx1fl/fl mice as compared to controls (37.44±6.5 vs 28.44±5.2 min, repsectively. n=7-9). Finally, respiratory arrest after induction of venous thromboembolism was delayed in both Panx1-/- (233±14 vs 190±9 s. n=10) or Pf4-Cre+Panx1fl/fl (349±70 vs 241±11 s. n=6-7) mice as compared to their controls.

Conclusion: Panx1 contributes to platelet aggregation in thrombus formation during hemostasis, arterial and venous thrombosis. As Panx1 channel inhibitors include a commonly-used food dye and FDA-approved drugs like probenecid and mefloquine, this finding may have important clinical and therapeutic implications.